

Polyhedral Cobalt(II) and Iron(II) Siloxanes: Synthesis and X-ray Crystal Structure of $[(\text{RSi}(\text{OH})\text{O}_2)\text{Co}(\text{OPMe}_3)]_4$ and $[(\text{RSiO}_3)_2(\text{RSi}(\text{OH})\text{O}_2)_4(\mu_3\text{-OH})_2\text{Fe}_8(\text{THF})_4]$ ($\text{R} = (2,6\text{-iPr}_2\text{C}_6\text{H}_3)\text{N}(\text{SiMe}_3)$)

Umesh N. Nehete,[†] Herbert W. Roesky,^{*,†} Hongping Zhu,[†] Sharanappa Nembenna,[†] Hans-Georg Schmidt,[†] Mathias Noltemeyer,[†] Dmitriy Bogdanov,[‡] and Konrad Samwer[‡]

Institut für Anorganische Chemie der Georg-August Universität, Göttingen, Tammannstrasse 4, 37077 Göttingen, Germany, and I. Physikalisches Institut, Universität Göttingen, Tammannstrasse 1, D-37077 Göttingen, Germany

Received May 27, 2005

The cobalt(II) and iron(II) siloxane compounds were prepared by the reaction of lipophilic N-bonded silanetriol **1** with metal silylamides $\text{M}[\text{N}(\text{SiMe}_3)_2]_2$ ($\text{M} = \text{Co}$ (**2**), Fe (**3**)) in a 1:1 and 3:4 molar ratio, respectively. A plot of $1/\chi$ versus temperature in the range of 2–300 K indicates the paramagnetic behavior of **2** and **3**. The composition and molecular structures of **2** and **3** were fully determined by IR, elemental analysis, and X-ray crystal structural analyses. Compound **2** possesses a pseudo-4-fold (S_4) symmetry, whereas **3** reveals an inversion center. Compound **2** represents a tetracobalt(II) drum while **3** exhibits an octairon(II) cage containing siloxane ligands.

Introduction

The metallasiloxanes containing the Si–O–M functional group ($\text{M} =$ main group or transition metal) is one of the most important structural units of inanimate nature. The various metal silicates are built up from such units, and the presence of metal in the siloxane framework not only makes these compounds thermally stable but also improves their catalytic and conducting properties. We have been utilizing the multi-functional N-bonded silanetriol $\text{RSi}(\text{OH})_3$ ($\text{R} = (2,6\text{-iPr}_2\text{C}_6\text{H}_3)\text{N}(\text{SiMe}_3)$) (**1**) for the preparation of various polyhedral metallasiloxanes with a high metal/silicon ratio.^{1,2}

Soluble metallasiloxanes may serve as model compounds for complex metallasilicate frameworks that either occur naturally or have been synthesized in the laboratory.³ Although, the molecular species are only models for covalently bonded transition metal–silica combinations they are an important source for structural parameters, which are in general not easily available for complex metallasilicate frameworks. Many industrially and commercially important processes are catalyzed by transition metal complexes immobilized on silica surfaces.⁴ For example cobalt- and iron-containing silicate frameworks include zeolites such as Co-ZSM-5 and

* Author to whom correspondence should be addressed. E-mail: hroesky@gwdg.de.

[†] Institut für Anorganische Chemie der Georg-August Universität.

[‡] I. Physikalisches Institut der Georg-August Universität.

- (1) (a) Chandrasekhar, V.; Murugavel, R.; Voigt, A.; Roesky, H. W. *Organometallics* **1996**, *15*, 918–922. (b) Murugavel, R.; Voigt, A.; Walawalkar, M. G.; Roesky, H. W. *Chem. Rev.* **1996**, *96*, 2205–2236. (c) Murugavel, R.; Chandrasekhar, V.; Roesky, H. W. *Acc. Chem. Res.* **1996**, *29*, 183–189. (d) Murugavel, R.; Bhattacharjee, M.; Roesky, H. W. *Appl. Organomet. Chem.* **1999**, *13*, 227–243. (e) Roesky, H. W.; Anantharaman, G.; Chandrasekhar, V.; Jancik, V.; Singh, S. *Chem. Eur. J.* **2004**, *10*, 4106–4114. (f) Feher, F. J.; Budzichowski, T. A. *Polyhedron* **1995**, *14*, 3239–3253. (g) Duchateau, R. *Chem. Rev.* **2002**, *102*, 3525–3542.
- (2) (a) Schmidbaur, H. *Angew. Chem.* **1965**, *77*, 206–216; *Angew. Chem., Int. Ed. Engl.* **1965**, *4*, 201–211. (b) Veith, M.; Vogelgesang, H.; Huch, V. *Organometallics* **2002**, *21*, 380–388. (c) Baerlocher, C.; Meier, W. M.; Olson, D. H. *Atlas of Zeolite Framework Types*, 5th ed.; Elsevier: Amsterdam, 2001. (d) Merz, K.; Block, S.; Schoenen, R.; Driess, M. *Dalton Trans.* **2003**, 3365–3369. (e) Walawalkar, M. G. *Organometallics* **2003**, *22*, 879–881.

- (3) (a) Voigt, A.; Murugavel, R.; Parisini, E.; Roesky, H. W. *Angew. Chem.* **1996**, *108*, 823–825; *Angew. Chem., Int. Ed. Engl.* **1996**, *35*, 748–750. (b) Voigt, A.; Walawalkar, M. G.; Murugavel, R.; Roesky, H. W.; Parisini, E.; Lubini, P. *Angew. Chem.* **1997**, *109*, 2313–2315; *Angew. Chem., Int. Ed. Engl.* **1997**, *36*, 2203–2205. (c) Voigt, A.; Murugavel, R.; Roesky, H. W. *Organometallics* **1996**, *15*, 5097–5101. (d) Nehete, U. N.; Chandrasekhar, V.; Anantharaman, G.; Roesky, H. W.; Vidovic, D.; Magull, J. *Angew. Chem.* **2004**, *116*, 3930–3932; *Angew. Chem., Int. Ed.* **2004**, *43*, 3842–3844. (e) Nehete, U. N.; Chandrasekhar, V.; Jancik, V.; Roesky, H. W.; Herbst-Irmer, R. *Organometallics* **2004**, *23*, 5372–5374. (f) Nehete, U. N.; Chandrasekhar, V.; Roesky, H. W.; Magull, J. *Angew. Chem.* **2005**, *117*, 285–288; *Angew. Chem., Int. Ed.* **2005**, *44*, 281–284.
- (4) (a) Pearce, R.; Patterson, W. R. *Catalysis and Chemical Processes*; Blackie and Son: Glasgow, 1981. (b) Seiyama, T.; Tanabe, K. *New Horizons in Catalysis*; Elsevier: Amsterdam, 1980. (c) Iwasawa, Y. *Tailored Metal Catalysts*; Reidel: Dordrecht, The Netherlands, 1986. (d) Thomas, C. L. *Catalytic Processes and Proven Catalysts*; Academic Press: New York, 1970. (e) Kaminsky, W.; Sinn, H. *Transition Metals and Organometallics as Catalysts for Olefin Polymerization*; Springer-Verlag: Heidelberg, 1988.

Fe-modified ZSM-5. The Co-ZSM-5 type catalysts have been found to possess a high activity and selectivity for NO decomposition in the presence of hydrocarbons, whereas the Fe-modified ZSM-5 has been important in the synthesis of phenol from benzene and N₂O.⁵ Nevertheless, due to the heterogeneous nature of the catalysts, the catalytic species are normally difficult to characterize, and the exact reactions occurring at such surfaces are remaining unclear. In these cases lipophilic metallasiloxanes may serve as useful models for silica-supported transition metal catalysts.^{1,6} Metallasiloxanes have also been envisaged as single-source precursors for modified zeolites.⁷ More recently, some of these metallasiloxanes have also been found to be useful in homogeneous catalysis reactions such as [RSiO₃TiOR¹]₄ [R = (2,6-*i*Pr₂C₆H₃)N(SiMe₃)] [R¹ = (Et, *i*Pr)] for the epoxidation of olefins.⁸

In previous papers, we reported the synthesis and single-crystal X-ray structures of zinc [(RSi(OH)O₂)Zn(THF)]₄⁹ and ferrous siloxanes [{(Me₃Si)₂NFe}₂{LFe}₂{O₃SiR}₂]₁₀ (L = 1,3-diisopropyl-4,5-dimethylimidazol-2-ylidene) using metal alkyl/amide complexes with kinetically stable amino-silanetriol. As a part of our continuing study of low-coordinate transition metal siloxanes, this paper describes the synthesis and X-ray crystal structures of [(RSi(OH)O₂)Co(OPMe₃)₄] (2) and [(RSiO₃)₂(RSi(OH)O₂)₄(μ₃-OH)₂Fe₈(THF)₄] (3) (R = (2,6-*i*Pr₂C₆H₃)N(SiMe₃)). Compound 2 represents the first example of a tetracobalt(II) drum containing siloxane ligands. Previously several methods were reported for the synthesis of cobalt(II)¹¹ and iron(II)¹² siloxanes starting from R₃SiO or silsesquioxane ligands.

Experimental Section

General Comments. All experimental manipulations were carried out under a dry nitrogen atmosphere, rigorously excluding air and moisture. The samples for spectral measurements were prepared in a drybox. Solvents were purified according to conven-

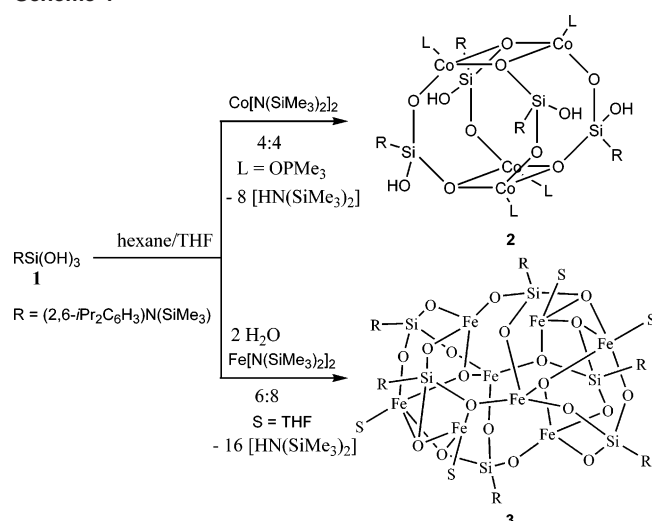
tional procedures and were freshly distilled prior to use. Silanetriol,¹³ Co[N(SiMe₃)₂]₂,^{14,15} and Fe[N(SiMe₃)₂]₂·THF¹⁶ were prepared according to the published procedures. Elemental analyses were performed by the Analytisches Labor des Instituts für Anorganische Chemie der Universität Göttingen. NMR spectra were recorded on Bruker Advance 500 MHz spectrometers. IR spectra were obtained on a Bio-Rad FTS-7 spectrometer as Nujol mulls. Mass spectra were obtained on a Finnigan MAT system 8230 and a Varian MAT CH5 mass spectrometer by EI-MS methods. Melting points were recorded on a HWS-SG 3000 apparatus and are uncorrected. Variable-temperature magnetic measurements were recorded using a SQUID magnetometer (Quantum Design). Samples were prepared in a glovebox by crushing single crystals. The crushed single crystals were restrained between the two halves of a gelatine capsule by inverting the top half.

Synthesis of [(RSi(OH)O₂)Co(OPMe₃)₄] [R = (2,6-*i*Pr₂C₆H₃)N(SiMe₃)] (2). Co[N(SiMe₃)₂]₂ (1.63 g, 4.28 mmol) in hexane (10 mL) was slowly added to a suspension of silanetriol (1.4 g, 4.28 mmol) in THF/hexane (2 mL, 5 mL). After the addition was completed, the reaction mixture was stirred for 24 h at room temperature. The green-colored solution slowly turned to greenish indigo. A solution of trimethylphosphine oxide (0.4 g, 4.34 mmol) in THF (20 mL) was added, and the stirring was continued for one more day. The volatile components were removed to obtain a blue solid. To this a mixture of toluene (10 mL) and THF (1 mL) was added. Blue-colored crystals of 2 were obtained at room temperature over a period of 2 weeks (0.88 g, 43%); mp. 196–198 °C; IR (Nujol): $\tilde{\nu}$ = 3381 (w), 2363 (w), 2254 (w), 2195 (m), 1924 (w), 1863 (w), 1797 (w), 1701 (w), 1653 (w), 1599 (m), 1579 (m), 1488 (m), 1439 (s), 1407 (s), 1361 (s), 1391 (s), 1249 (s), 1182 (s), 1104 (s), 1027 (s), 933 (s), 910 (s), 880 (s), 838 (s), 803 (s), 755 (s), 685 (m), 641 (w), 618 (w), 599 (m), 546 (m), 489 (m), 440 (m) cm⁻¹. Elemental analysis calcd (%) C₇₂H₁₄₄Co₄N₄O₁₆P₄Si₈ (1906.24): C, 45.37; H, 7.61; N, 2.94. Found: C, 44.76; H, 7.89; N, 3.12.

Synthesis of [(RSiO₃)₂(RSi(OH)O₂)₄(μ₃-OH)₂Fe₈(THF)₄] (3). The liquid Fe[N(SiMe₃)₂]₂·THF (2.6 g, 5.79 mmol) was slowly added to a suspension of RSi(OH)₃ (1.4 g, 4.28 mmol) in THF/

- (5) (a) Sun, T.; Fokema, M. D.; Ting, J. Y. *Catal. Today* **1997**, *33*, 251–261. (b) Ivanov, A. A.; Chernyavsky, V. S.; Gross, M. J.; Kharitonov, A. S.; Uriarte, A. K.; Panov, G. I. *Appl. Catal. A* **2003**, *249*, 327–343. (c) Ivanov, D. P.; Sobolev, V. I.; Pirutko, L. V.; Panov, G. I. *Adv. Synth. Catal.* **2002**, *344*, 986–995. (d) Ivanov, D. P.; Rodkin, M. A.; Dubkov, K. A.; Kharitonov, A. S.; Panov, G. I. *Kinet. Catal.* **2000**, *41*, 771–775.
- (6) (a) Feher, F. *J. Am. Chem. Soc.* **1986**, *108*, 3850–3852. (b) Edlmann, F. T. *Angew. Chem.* **1992**, *104*, 600–601; *Angew. Chem., Int. Ed.* **1992**, *31*, 586–587. (c) Gouzyr, A. I.; Wessel, H.; Barnes C. E.; Roesky, H. W.; Teichert, M.; Usón, I. *Inorg. Chem.* **1997**, *36*, 3392–3393. (d) Winkhofer, N.; Roesky, H. W.; Noltemeyer, M.; Robinson, W. T. *Angew. Chem.* **1992**, *104*, 670–671; *Angew. Chem., Int. Ed. Engl.* **1992**, *31*, 599–601.
- (7) (a) Murugavel, R.; Shete, V. S.; Baheti, K.; Davis, P. J. *Organomet. Chem.* **2001**, *625*, 195–199. (b) Murugavel, R.; Davis, P.; Shete, V. S. *Inorg. Chem.* **2003**, *42*, 4696–4706. (c) Terry, K. W.; Lugmair, C. G.; Gantzel, P. K.; Tilley, T. D. *Chem. Mater.* **1996**, *8*, 274–280. (d) Su, K.; Tilley, T. D.; Sailor, M. J. *J. Am. Chem. Soc.* **1996**, *118*, 3459–3468.
- (8) (a) Fujiwara, M.; Wessel, H.; Park, H.-S.; Roesky, H. W. *Tetrahedron* **2002**, *58*, 239–243. (b) Fujiwara, M.; Wessel, H.; Park, H.-S.; Roesky, H. W. *Chem. Mater.* **2002**, *14*, 4975–4981. (c) Abbenhuis, H. C. L. *Chem. Eur. J.* **2000**, *6*, 25–32.
- (9) Anantharaman, G.; Roesky, H. W.; Schmidt, H.-G.; Noltemeyer, M.; Pinkas, J. *Inorg. Chem.* **2003**, *42*, 970–973.
- (10) Nehete, U. N.; Anantharaman, G.; Chandrasekhar, V.; Murugavel, R.; Walawalker, M. G.; Roesky, H. W.; Vidovic, D.; Magull, J.; Samwer, K.; Sass, B. *Angew. Chem.* **2004**, *116*, 3920–3923; *Angew. Chem., Int. Ed.* **2004**, *43*, 3832–3835.
- (11) (a) Olmstead, M. M.; Sigel, G. A.; Hope, H.; Xu, X.; Power, P. P. *J. Am. Chem. Soc.* **1985**, *107*, 8087–8091. (b) Sigel, G. A.; Bartlett, R. A.; Decker, D.; Olmstead, M. M.; Power, P. P. *Inorg. Chem.* **1987**, *26*, 1773–1780. (c) Chesnokova, T. A.; Zhezlova, E. V.; Kornev, A. N.; Fedotova, Y. V.; Zakharov, L. N.; Fukin, G. K.; Kursky, Y. A.; Mushina, T. G.; Domrachev, G. A. *J. Organomet. Chem.* **2002**, *642*, 20–31. (d) Abrahams, I.; Lazell, M.; Motevallii, M.; Simon, C.; Sullivan, A. C. *Chem. Heterocycl. Compd. (N.Y.)* **1999**, *35*, 954–964. (e) Ackermann, H.; Weller, F.; Dehnicke, K. *Z. Naturforsch. B* **2000**, *55*, 448–451. (f) Yoshimitsu, S.; Hikichi, S.; Akita, M. *Organometallics* **2002**, *21*, 3762–3773. (g) Abrahams, I.; Motevallii, M.; Shah, D.; Sullivan, A. C.; Thornton, P. *Chem. Commun.* **1993**, 1514–1515. (h) Hursthouse, M. B.; Mazid, M. A.; Motevallii, M.; Sanganee, M.; Sullivan, A. C. *J. Organomet. Chem.* **1990**, *381*, C43–C46. (i) Becker, B.; Radacki, K.; Konitz, A.; Wojnowski, W. *Z. Anorg. Allg. Chem.* **1995**, *621*, 904–908.
- (12) (a) Kornev, A. N.; Chesnokova, T. A.; Semenov, V. V.; Zhezlova, E. V.; Zakharov, L. N.; Klapshina, L. G.; Domrachev, G. A.; Rusakov, V. S. *J. Organomet. Chem.* **1997**, *547*, 113–119. (b) Liu, F.; John, K. D.; Scott, B. L.; Baker, R. T.; Ott, K. C.; Tumas, W. *Angew. Chem.* **2000**, *112*, 3257–3260; *Angew. Chem., Int. Ed.* **2000**, *39*, 3127–3130. (c) Esposito, V.; Solari, E.; Floriani, C. *Inorg. Chem.* **2000**, *39*, 2604–2613.
- (13) Winkhofer, N.; Voigt, A.; Dorn, H.; Roesky, H. W.; Steiner, A.; Stalke, D.; Reller, A. *Angew. Chem.* **1994**, *106*, 1414–1416; *Angew. Chem., Int. Ed. Engl.* **1994**, *33*, 1352–1354.
- (14) Andersen, R. A.; Faegri, K., Jr.; Green, J. C.; Haaland, A.; Lappert, M. F.; Leung, W.; Rypdal, K. *Inorg. Chem.* **1988**, *27*, 1782–1786.
- (15) Bürger, H.; Wannagat, U. *Monatsh. Chem.* **1963**, *94*, 1007–1012.
- (16) Olmstead, M. M.; Power, P. P.; Shoner, S. C. *Inorg. Chem.* **1991**, *30*, 2547–2551.

Scheme 1



hexane (4 mL, 25 mL) at room temperature. After stirring for 1 h, the color of the solution turned from green to greenish blue. The resulting clear solution was stirred for another 48 h at room temperature and then heated to reflux for 1 h. The solvents and hexamethyldisilazane were removed in vacuo to give a greenish blue product. This was recrystallized from a mixture of toluene and THF (8 mL, 2 mL). The reddish yellow crystals of **3** were obtained at $-26\text{ }^\circ\text{C}$ over a period of 2 weeks (0.42 g, 24%); mp. $210\text{--}212\text{ }^\circ\text{C}$; IR (Nujol): $\tilde{\nu} = 3652$ (w), 3265 (w), 1320 (w), 1259 (m), 1249 (s), 1184 (m), 1101 (m), 1044 (s), 1018 (m), 969 (s), 944 (s), 905 (s), 840 (s), 802 (s), 755 (w), 722 (m), 686 (w), 642 (w), 569 (m), 542 (m), 478 (m) cm^{-1} . Elemental analysis calcd (%) (toluene and THF molecules were removed by drying under vacuum) for $\text{C}_{90}\text{H}_{162}\text{Fe}_8\text{N}_6\text{O}_{20}\text{Si}_{12}$ (2432.06): C, 44.45; H, 6.71; N, 3.46. Found: C, 44.19; H, 6.96; N, 3.30.

X-ray Structure Determination of 2 and 3. Data for the structure were collected on a Bruker three-circle diffractometer equipped with a SMART 6000 CCD detector. Intensity measurements were performed on a rapidly cooled crystal. The structures were solved by direct methods (SHELXS-97)¹⁷ and refined with all data by full-matrix least squares on F^2 .¹⁸ The hydrogen atoms of C–H bonds were placed in idealized positions and refined isotropically with riding model, whereas the non-hydrogen atoms were refined anisotropically.

Results and Discussion

The addition of $\text{Co}[\text{N}(\text{SiMe}_3)_2]_2$ in hexane to a suspension of $\text{RSi}(\text{OH})_3$ (**1**) in THF/hexane mixture at room temperature in the presence of trimethylphosphine oxide L affords **2** in moderate yield (Scheme 1).

The reaction proceeds by elimination of eight molecules of $\text{HN}(\text{SiMe}_3)_2$ with a concomitant Co–O–Si bond formation containing an unreacted OH group on each silicon atom. The use of the auxiliary coordinating ligand L allowed the isolation of the cobalt(II) siloxane **2** as a crystalline product. Compound **2** is highly soluble in common organic solvents; **2** has been unambiguously characterized by means of analytical, spectroscopic, and single-crystal diffraction stud-

ies. The pure crystalline solid of **2** is thermally quite stable up to its melting point of $196\text{--}198\text{ }^\circ\text{C}$, after which its color slowly turns to brown upon decomposition. However, no peak attributable to the molecular ion of **2** can be observed in the EI or other mass spectrometric methods. Only smaller fragment ion peaks are found. The IR spectrum exhibited a weak absorption at 3381 cm^{-1} , which is comparable with that of the OH stretching frequency of the silanol groups (3344 cm^{-1}).¹³ The IR spectra of **2** and **3** are dominated by the typical M–O–Si stretching frequencies observed in the range of $900\text{--}1000\text{ cm}^{-1}$.

Structural Description of 2. The blue color crystals of **2** were obtained by slow cooling of its saturated solution in toluene and THF at room temperature over a period of 2 weeks. Compound **2** crystallizes in the monoclinic space group $P1(1)/c$, with two molecules in the asymmetric unit. Selected metric parameters of **2** are summarized in Table 1. The core structure of **2** is given in Figure 1. The molecular structure of **2** can be described as a polyhedral drum-like architecture with a pseudo-4-fold (S_4) symmetry. The core structure consists of four cobalt, four silicon, and eight oxygen atoms. Importantly, every silicon atom has one unreactive Si–OH group. The $\text{Co}_4\text{O}_8\text{Si}_4$ core is surrounded by eight bridging oxo ligands, four double bridging ($\mu\text{-O}$), and four triply bridged ($\mu_3\text{-O}$) oxygen atoms. An alternative way of viewing **2** is that it contains two puckered $\text{Co}_2\text{O}_4\text{Si}_2$ [$\text{Co}(1)\text{--O}(31)\text{--Si}(3)\text{--O}(33)\text{--Co}(4)\text{--O}(12)\text{--Si}(1)\text{--O}(13)$, $\text{Co}(2)\text{--O}(43)\text{--Si}(4)\text{--O}(42)\text{--Co}(3)\text{--O}(21)\text{--Si}(2)\text{--O}(23)$] boat-like eight-membered rings that are fused together by four Co–O [Co(1)–O(42), Co(2)–O(33), Co(3)–O(13), Co(4)–O(23)] bonds. Interestingly, this arrangement leads to the formation of two almost planar four-membered Co_2O_2 rings [Co(1)–O(42)–Co(3)–O(13), Co(2)–O(23)–Co(4)–O(33)], and the cobalt atoms of one ring are connected with the oxygens of the second one.

Each cobalt is tetracoordinate with its coordination environment made up of only oxygen atoms, in which OPMe_3 takes up the fourth coordination side. The coordination geometry around both the cobalt and the silicon centers is nearly tetrahedral. The shortest Co–O and Si–O distances are seen for Co(1)–O(31) [$1.937(8)\text{ \AA}$] and Si(2)–O(21) bonds [$1.600(8)\text{ \AA}$] while the longest distances are observed for Co(1)–O(42) [$2.016(9)\text{ \AA}$] and Si(1)–O(11) bonds [$1.640(9)\text{ \AA}$], respectively. The bond lengths involving the μ_3 oxygen centers are found to be longer {Co(1)–O(42) [$2.016(9)\text{ \AA}$], Co(2)–O(23) [$2.013(8)\text{ \AA}$], Co(3)–O(13) [$2.011(9)\text{ \AA}$], Co(4)–O(33) [$1.988(8)\text{ \AA}$]} than the corresponding distances involving the μ oxygens {Co(1)–O(31) [$1.937(8)\text{ \AA}$], Co(2)–O(43) [$1.944(8)\text{ \AA}$], Co(3)–O(21) [$1.938(8)\text{ \AA}$], Co(4)–O(12) [$1.967(8)\text{ \AA}$]}. A similar range of bond distances was also observed in the case of other cobalt(II) siloxanes that have been reported earlier. Thus, in [$\{\text{Co}_3(p\text{-tert-butylcalix}[4]\text{areneOSiMe}_3)_2(\text{THF})\}\cdot 5\text{Ph-Me}$],^{11a} [$\{\text{Co}(\text{OSiPh}_3)_2(\text{THF})_2\}_2$],^{11b} and [$\{((\text{Me}_3\text{Si})_3\text{SiO})_2\text{-Co}\}_2$]^{11c} contain a four-membered Co_2O_2 ring with the average Co–O bond distance of $1.985(1)\text{ \AA}$, $1.988(3)\text{ \AA}$, and $1.952(8)\text{ \AA}$, respectively. The O–Co–O bond angles within the Co_2O_2 rings are around 90° and reveal the almost perfect

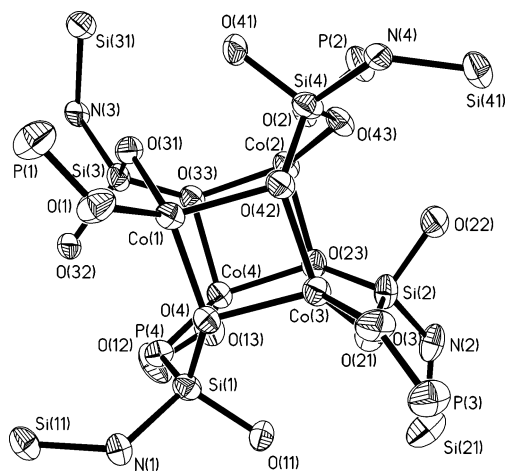
(17) Sheldrick, G. M. SHELXS-97, Program for Structure Solution. *Acta Crystallogr. Sect. A* **1990**, *46*, 467–473.

(18) Sheldrick, G. M. SHELXL-97, Program for Crystal Structure Refinement; University of Göttingen: Göttingen, Germany, 1997.

Table 1. Crystal Data and Structure Refinement for **2** and **3**

	2	3 C ₆₇ H ₈
formula	C ₇₂ H ₁₄₄ Co ₄ N ₄ O ₁₆ P ₄ Si ₈	C ₁₄₈ H ₂₄₂ Fe ₈ N ₆ O ₂₄ Si ₁₂
fw	1906.23	3273.32
crystal system	monoclinic	triclinic
space group	<i>P</i> 1(1)/ <i>c</i>	<i>P</i> $\bar{1}$
temp, K	133(2)	133(2)
λ , Å	0.71073	0.71073
<i>a</i> , Å	28.705(6)	16.129(13)
<i>b</i> , Å	27.685(6)	16.787(13)
<i>c</i> , Å	29.579(6)	17.464(14)
α , deg	90	61.55(4)
β , deg	106.41(3)	81.35(5)
γ , deg	90	86.55(5)
<i>V</i> , Å ³	2255(1)	4109.9(6)
<i>Z</i>	8	1
ρ_{calcd} , g/cm ³	1.123	1.320
μ , mm ⁻¹	0.769	0.837
<i>F</i> (000)	8096	1734
crystal size, mm ³	0.30 × 0.20 × 0.20	0.20 × 0.20 × 0.10
θ range for data collection, deg	1.60 to 24.92	1.87 to 24.79
index ranges	−32 ≤ <i>h</i> ≤ 33 −31 ≤ <i>k</i> ≤ 32 −34 ≤ <i>l</i> ≤ 34	−18 ≤ <i>h</i> ≤ 17 −19 ≤ <i>k</i> ≤ 19 −20 ≤ <i>l</i> ≤ 20
no. of rflns collected	60890	76145
no. of independent rflns (<i>R</i> _{int})	30611 (0.1441)	13591 (0.1561)
no. of data/restraints/parameters	30611/2771/2032	13591/0/916
GOF on <i>F</i> ²	0.697	0.927
<i>R</i> 1, ^a <i>wR</i> 2 ^b (<i>I</i> > 2σ(<i>I</i>))	0.0676, 0.1319	0.0693, 0.1230
<i>R</i> 1, ^a <i>wR</i> 2 ^b (all data)	0.2562, 0.1844	0.1466, 0.1433
largest diff. peak/hole, e [−] Å ^{−3}	0.777/−0.382	0.682/−0.491

$${}^a R = \sum ||F_o| - |F_c|| / \sum |F_o|. \quad {}^b wR2 = [\sum w(F_o^2 - F_c^2)^2 / \sum w(F_o^2)]^{1/2}.$$

**Figure 1.** ORTEP diagram of core **2** with 50% probability. Most of the substituents on silicon and cobalt atoms are omitted for the sake of clarity.

rectangular geometry of the four-membered rings. The Co(1)–Co(3) and Co(2)–Co(4) distances 2.890(3) Å and 2.889(3) Å are also very close to the reported ones.^{11a}

The reaction of Fe[N(SiMe₃)₂]₂ with the N-bonded silanetriol RSi(OH)₃ (**1**) in a 6:8 stoichiometric ratio affords the polyhedral octanuclear iron(II) siloxane **3** in 24% yield (Scheme 1). The isolation of the crystalline product can be achieved in the presence of a Lewis base such as THF. During the course of the reaction a part of silanetriol undergoes self-condensation to generate the disiloxanetetrol [(RSi(OH)₂)₂O] and water. This process of self-condensation appears to be mediated by the iron(II) amide. It may be noted that we had earlier observed a similar condensation of two silanetriol molecules in the presence of hydrazine.¹⁹ Moreover, in the presence of Fe[N(SiMe₃)₂]₂ the OH group of

water is capped by three Fe(II) centers by loss of one molecule of HN(SiMe₃)₂. Thus, the overall reaction takes place among six molecules of silanetriol, eight molecules of Fe[N(SiMe₃)₂]₂, and two molecules of water which leads to the formation of [(RSiO₃)₂(RSi(OH)O₂)₄(μ₃-OH)₂Fe₈(THF)₄] (R = (2,6-*i*Pr₂C₆H₃N(SiMe₃)) (**3**) by loss of 16 molecules of HN(SiMe₃)₂. Therefore, **3** contains an unreacted OH group on four silanetriol molecules, and two OH groups are trapped by three Fe(II) centers. The low yield of **2** may be due to the water formation in this system. Selected bond lengths and bond angles for **2** and **3** are given in Table 2.

Albeit the above statement is consistent with the stoichiometry of the reactants, we were not able to resolve the hydroxyl protons in the molecular structure of **3** due to the proximity of high electron density metal atoms. The formation of **3** is insensitive to the slight variations of reactant stoichiometry. Thus, the equimolar quantity of the reactants also leads to the same product formation of **3**. A remarkable feature of the Fe(II) siloxane **3** is its high thermal stability. It is stable up to its melting point of 210–212 °C at which the color of the compound turns into reddish brown. Moreover, no peak attributable to the molecular ion of **3** can be observed in the EI or other mass spectrometric methods. Compound **3**, like **2** discussed above, is highly lipophilic and is soluble in various organic solvents such as benzene, toluene, and THF. Compounds **2** and **3** are paramagnetic and give broad resonances in the NMR spectra. OH stretching vibrations are observed at 3652 and 3265 cm^{−1} in the IR

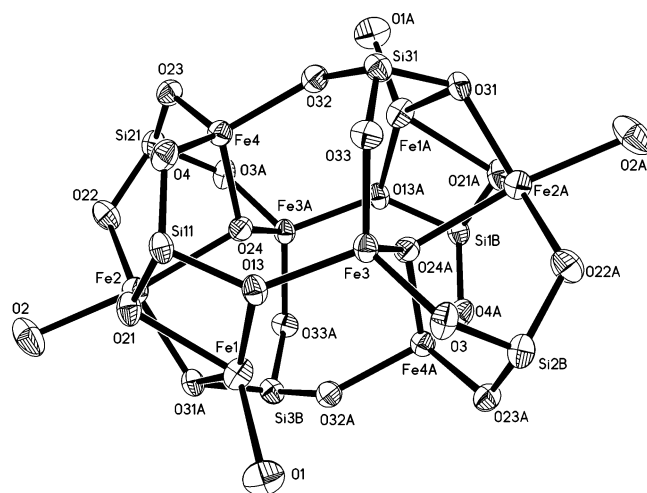
(19) Murugavel, R.; Böttcher, P.; Voigt, A.; Walawalkar, M. G.; Roesky, H. W.; Parisini, E.; Teichert, M.; Noltemeyer, M. *Chem. Commun.* **1996**, 2417–2418.

Table 2. Selected Bond Lengths (Å) and Bond Angles (°) for **2** and **3**

Compound 2			
Co(1)–O(13)	1.967(8)	O(13)–Co(1)–O(42)	87.2(3)
Co(1)–O(31)	1.937(8)	O(31)–Co(1)–O(42)	106.9(3)
Co(2)–O(33)	1.961(9)	O(33)–Co(2)–O(23)	86.3(3)
Co(2)–O(43)	1.944(8)	O(43)–Co(2)–O(23)	106.9(3)
Co(1)–Co(3)	2.890(3)	O(12)–Si(1)–O(13)	109.8(4)
Si(1)–O(11)	1.640(9)	O(13)–Si(1)–O(11)	106.5(4)
Si(1)–O(13)	1.624(9)	O(21)–Si(2)–O(22)	112.2(5)
Si(2)–O(22)	1.632(9)	O(1)–Co(1)–O(42)	117.9(4)
Si(3)–O(32)	1.636(9)	O(1)–Co(1)–O(13)	111.3(3)
Co(1)–O(42)	2.016(9)	O(33)–Co(2)–O(2)	108.3(4)
Co(1)–O(1)	1.959(8)	O(2)–Co(2)–O(23)	118.6(3)
Co(2)–O(23)	2.013(8)	O(12)–Si(1)–O(11)	113.7(4)
Co(2)–O(2)	1.969(8)	O(21)–Si(2)–O(23)	109.6(5)
Co(2)–Co(4)	2.889(3)	O(23)–Si(2)–O(22)	106.3(5)
Si(1)–O(12)	1.605(8)		
Si(2)–O(21)	1.600(8)		
Si(2)–O(23)	1.632(9)		
Si(4)–O(41)	1.622(9)		
Compound 3			
Fe(1)–O(1)	2.038(4)	O(1)–Fe(1)–O(31A)	119.54(18)
Fe(1)–O(31A)	2.111(4)	O(1)–Fe(1)–O(13)	96.04(18)
Fe(1)–O(13)	2.116(4)	O(31A)–Fe(1)–O(13)	142.88(16)
Fe(1)–O(21)	2.150(4)	O(1)–Fe(1)–O(21)	121.54(17)
Fe(2)–O(22)	1.954(4)	O(31A)–Fe(1)–O(21)	80.38(16)
Fe(2)–O(21)	1.960(4)	O(13)–Fe(1)–O(21)	71.48(16)
Fe(2)–O(31A)	1.971(4)	O(22)–Fe(2)–O(21)	136.31(19)
Fe(2)–O(2)	2.122(4)	O(22)–Fe(2)–O(31A)	134.66(19)
Fe(2)–O(24)	2.201(4)	O(21)–Fe(2)–O(31A)	88.80(17)
Fe(3)–O(33)	1.845(4)	O(22)–Fe(2)–O(24)	86.76(17)
Fe(3)–O(3)	1.862(4)	O(21)–Fe(2)–O(24)	90.40(17)
Fe(3)–O(24A)	1.883(4)	O(31A)–Fe(2)–O(24)	89.00(16)
Fe(3)–O(13)	1.915(4)	O(33)–Fe(3)–O(3)	119.00(2)
Fe(4)–O(4)	1.860(4)	O(3)–Fe(3)–O(24A)	99.05(18)
Fe(4)–O(23)	1.865(4)	O(33)–Fe(3)–O(13)	109.80(18)
Fe(4)–O(24)	1.892(4)	O(4)–Fe(4)–O(23)	119.77(18)
Fe(4)–O(32)	1.920(4)	O(23)–Fe(4)–O(24)	99.27(19)
Si(11)–O(4)	1.624(4)	O(23)–Fe(4)–O(32)	111.6(18)
Si(11)–O(21)	1.637(5)	O(3A)–Si(21)–O(23)	111.3(2)
Si(11)–O(13)	1.659(4)	O(3A)–Si(21)–O(22)	107.3(2)
Si(21)–O(3A)	1.611(4)	O(33)–Si(31)–O(32)	113.6(2)
Si(21)–O(23)	1.614(5)	Si(31)–O(33)–Fe(3)	123.9(2)
Si(21)–O(22)	1.688(4)	Si(21)–O(23)–Fe(4)	118.7(2)
Si(31)–O(33)	1.612(4)	Si(11)–O(4)–Fe(4)	122.7(2)
Si(31)–O(32)	1.642(5)	Si(21)–O(22)–Fe(2)	127.5(3)
Si(31)–O(31)	1.647(4)	Si(21A)–O(3)–Fe(3)	119.1(2)
		Si(31)–O(32)–Fe(4)	133.9(2)

spectrum of **3**. An analogous OH group absorption was observed in a titanium silicate.²⁰

Structural Description of 3. Single crystals of **3** suitable for X-ray structural analysis were obtained from a mixture of toluene and THF at $-26\text{ }^{\circ}\text{C}$ over a period of 2 weeks. Compound **3** crystallizes in the triclinic space group $P\bar{1}$, along with six molecules of toluene in the asymmetric unit. Selected metric parameters of **3** are given in Table 1. The molecular structure of **3** is made up of an $\text{Fe}_8\text{Si}_6\text{O}_{20}$ core, with an inversion center (Figure 2). The core structure of **3** contains two symmetry-related tetranuclear iron(II) units. Each of these $\text{Fe}_4\text{Si}_3\text{O}_{10}$ units contains four iron centers, one SiO_3 subunit, two Si(OH)O_2 subunits, and one (μ_3 -OH) group. Thus, there are three Fe_2SiO_3 [$\text{Fe}(2)\text{--O}(31\text{A})\text{--Si}(3\text{B})\text{--O}(33\text{A})\text{--Fe}(3\text{A})\text{--O}(24)$; $\text{Fe}(2)\text{--O}(22)\text{--Si}(21)\text{--O}(3\text{A})\text{--Fe}(3\text{A})\text{--O}(24)$; $\text{Fe}(2)\text{--O}(22)\text{--Si}(21)\text{--O}(23)\text{--Fe}(4)\text{--O}(24)$] six-membered rings, two $\text{Fe}_2\text{Si}_2\text{O}_4$ [$\text{Fe}(2)\text{--}$

**Figure 2.** ORTEP diagram of core **3** with 50% probability. Most of the substituents on silicon and iron atoms are omitted for the sake of clarity.

$\text{O}(31\text{A})\text{--Si}(3\text{B})\text{--O}(33\text{A})\text{--Fe}(3\text{A})\text{--O}(3\text{A})\text{--Si}(21)\text{--O}(22)$; $\text{Fe}(2)\text{--O}(22)\text{--Si}(21)\text{--O}(23)\text{--Fe}(4)\text{--O}(4)\text{--Si}(11)\text{--O}(21)$] eight-membered rings, and one FeSiO_2 [$\text{Fe}(1)\text{--O}(13)\text{--Si}(11)\text{--O}(21)$] four-membered ring. Both of the $\text{Fe}_4\text{Si}_3\text{O}_{10}$ units are fused together to generate two new [$\text{Fe}(4)\text{--O}(32)\text{--Si}(31)\text{--O}(33)\text{--Fe}(3)\text{--O}(13)\text{--Si}(11)\text{--O}(4)$; $\text{Fe}(3\text{A})\text{--O}(13\text{A})\text{--Si}(1\text{B})\text{--O}(4\text{A})\text{--Fe}(4\text{A})\text{--O}(32\text{A})\text{--Si}(3\text{B})\text{--O}(33\text{A})$] eight-membered rings, which leads to the assembly of the cage structure. An interesting feature of **3** is the coordination environment around the iron centers. Thus, there are three iron centers [$\text{Fe}(1)$, $\text{Fe}(3\text{A})$, $\text{Fe}(4)$] with nearly tetrahedral geometry and one $\text{Fe}(2)$ with a trigonal bipyramidal geometry. Two of these iron atoms [$\text{Fe}(3\text{A})$, $\text{Fe}(4)$] are surrounded by four oxygen atoms, whereas the remaining two [$\text{Fe}(1)$, $\text{Fe}(2)$] complete their coordination sphere by accepting an oxygen atom each from the THF molecules. Another interesting aspect of **3** is the presence of two different kinds of oxygen environments. Thus, there are six dicoordinate oxygen atoms that bridge Si and Fe atoms [$\text{O}(22)$, $\text{O}(23)$, $\text{O}(3\text{A})$, $\text{O}(33\text{A})$, $\text{O}(32\text{A})$, $\text{O}(4)$]. The angles at all these oxygen atoms are much less than 180° , the largest being at $\text{O}(32)$ (133.9°) and the smallest at $\text{O}(23)$ (118.7°). The remaining four tricoordinate oxygen atoms that cap each one silicon and two iron atoms [$\text{O}(31\text{A})$, $\text{O}(21)$, $\text{O}(13)$] or cap three iron centers [$\text{O}(24)$].

The Si–O bond distances fall in a narrow range from 1.611(4) Å to 1.688(4) Å for $\text{Si}(21)\text{--O}(3\text{A})$ and $\text{Si}(21)\text{--O}(22)$. The Si–O bond lengths $\text{Si}(11)\text{--O}(13)$, 1.659(4) Å and $\text{Si}(21)\text{--O}(22)$, 1.688(4) Å to which a hydrogen atom is attached, are longer than the other two Si–O bond distances around $\text{Si}(11)$ [average 1.631(4) Å] and $\text{Si}(21)$ [average 1.613(4) Å]. The latter Si–O distances are almost equal to those observed in $[(\text{RSi}(\text{OH})\text{O}_2)_6\text{Ti}_4(\mu_3\text{-O})_2]\cdot 2\text{THF}$.²⁰ The Fe–O bond distances range from 1.845(4) Å to 2.201(4) Å for $\text{Fe}(3)\text{--O}(33)$ and $\text{Fe}(2)\text{--O}(24)$, while those involving the μ oxygens are at the short end of the range 1.845(4) Å to 1.954(4) Å for $\text{Fe}(3)\text{--O}(33)$ and $\text{Fe}(2)\text{--O}(22)$, and those to the μ_3 oxygens are the longest $\text{Fe}(3)\text{--O}(13)$, 1.915(4) Å and $\text{Fe}(1)\text{--O}(21)$, 2.150(4) Å. The similar range of bond distances is also observed for coordinated THF molecules

(20) Voigt, A.; Murugavel, R.; Montero, M. L.; Wessel, H.; Liu, F.; Roesky, H. W.; Usón, I.; Albers, T.; Parisini, E. *Angew. Chem.* **1997**, *109*, 1020–1022; *Angew. Chem., Int. Ed. Engl.* **1997**, *36*, 1001–1003.

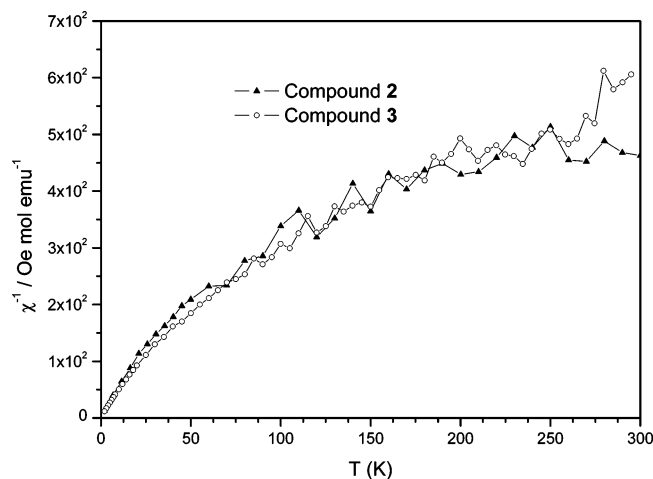


Figure 3. Plot of $1/\chi$ (Oe mol/emu) vs T (K) for **2** and **3**.

2.038(4) Å to 2.122(5) Å for Fe(1)–O(1) and Fe(2)–O(2). As would be expected, the longest Fe–O bond distances are to the capping (μ_3 -OH) hydroxide (Fe(3)–O(24A), 1.883(4) Å; Fe(2)–O(24), 2.201(4) Å). To the best of our knowledge such a structural variation within a single molecule is quite remarkable and unique. The metric parameters of **3** are quite normal and are analogous to those found in earlier examples $\{[(\text{Me}_3\text{Si})_3\text{SiOFe}\{\mu\text{-OSi}(\text{SiMe}_3)_3\}_2\text{-Na}(\text{DME})]\}$ (1.894(2)–1.910(2) Å);^{12a} $\{[(\text{C}_3\text{H}_9)_7\text{Si}_7\text{O}_{11}\text{-}(\text{OSiMe}_3)\text{Fe}(\text{dcpe})]\}$ (1.866(2)–1.873(3) Å);^{12b} $\{[(\text{Me}_3\text{-Si})_3\text{SiO}]_2\text{Fe}(2,2'\text{-dipyridyl})]\}$ (1.863(10)–1.899(10) Å);^{11c}

$\{[(\text{Me}_3\text{Si})_2\text{NFe}]_2\{\text{LFe}\}_2\{\text{O}_3\text{SiR}\}_2\}$ (L = 1,3-diisopropyl-4,5-dimethylimidazol-2-ylidene) (1.891(2)–2.143(2) Å).¹⁰

Magnetic Measurements of 2 and 3. Magnetic susceptibility measurements of crystalline samples of **2** and **3** were carried out in order to compare their behavior. Figure 3 shows a plot of $1/\chi$ versus temperature in the range of 2–300 K. This indicates the paramagnetic behavior for both compounds.

Conclusion

In summary, we report the synthesis and structural characterization of two novel tetrameric cobalt and octameric iron siloxanes, in which the cobalt and iron atoms are in formal oxidation state of +II. Compounds **2** and **3** contain the M/Si ratio of 4:4 and 8:6, respectively. A plot of $1/\chi$ versus temperature reveals the paramagnetic behavior for both compounds. By taking an advantage of reactive Si–OH units in these molecules, we are currently engaged in the synthesis of new hetero-trimetallic compounds.

Acknowledgment. We thank the Deutsche Forschungsgemeinschaft, the Göttinger Akademie der Wissenschaften, and the Fonds der Chemischen Industrie for funding.

Supporting Information Available: X-ray data (CIF) for **2** and **3**. This material is available free of charge via Internet at <http://pubs.acs.org>.

IC050859N